

Dielectric-loaded plasmonic nanoantenna arrays: A metamaterial with tuneable optical properties

W. Dickson, G. A. Wurtz, P. Evans, D. O'Connor, R. Atkinson, R. Pollard, and A. V. Zayats
Centre for Nanostructured Media, IRCEP, The Queen's University of Belfast, Belfast, BT7 1NN, United Kingdom
 (Received 13 February 2007; revised manuscript received 7 July 2007; published 11 September 2007)

The optical properties of metallic nanorod arrays acting as plasmonic nanoantennas have been studied. Large area arrays consisting of bare Au nanorods of diameter and length tuneable in the range of 20–40 and 200–400 nm, respectively, and spacing of about 40–100 nm have been electrochemically fabricated using templates of anodized nanoporous aluminium oxide. We demonstrate a very strong sensitivity of their resonant optical properties to both the presence of a dielectric load (which is much smaller than the wavelength of the resonant electromagnetic radiation) and modification of the refractive index of this load. This allows us to finely tune the spectral position of the plasmonic resonance of the nanoantenna arrays throughout the visible spectral range from about 550 to 800 nm with a sensitivity better than 3 Å per 1 nm thickness of the dielectric load. Such dielectric-loaded plasmonic nanoantenna arrays represent a type of anisotropic metallodielectric metamaterials with fully adjustable optical properties for imaging, sensing, and nonlinear optical applications.

DOI: [10.1103/PhysRevB.76.115411](https://doi.org/10.1103/PhysRevB.76.115411)

PACS number(s): 78.67.-n, 78.20.-e, 73.20.Mf

I. INTRODUCTION

The optical properties of one-dimensional nanostructures (nanowires and nanorods) provide an opportunity for novel applications in photonics and optoelectronics where enhanced functionality is required. Silica and semiconductor nanowires act as subwavelength dielectric waveguides at optical communication wavelengths.^{1,2} Semiconductor nanowires have been used to fabricate light-emitting diodes and achieve strong electromagnetic confinement for nanoscale ultraviolet lasing and photodetection as well as sensing applications.^{2–4}

Metallic one-dimensional structures are of particular interest as they support optical resonances at specific frequencies which results in the enhancement of their interaction with light similar to radio-frequency antennas.^{5–7} These resonances are plasmonic in nature as they are related to the coherent coupling of free electrons and photons. Optical plasmonic antennas find numerous applications including sensors based on enhanced Raman scattering, field enhancement effects for nonlinear optical applications, optical tags, near-field scanning optical microscopy, light coupling to single quantum objects, and negative refraction in nanowire composites.^{5–15}

In contrast to the previously reported studies of metallic nanoantennas placed on the substrate, this work deals with electrochemically grown, large area arrays consisting of standing Au nanorods of controllable diameter (20–40 nm), length (200–400 nm), and interrod spacing (40–100 nm). The nanorods have been partially covered with a dielectric layer to tune the resonance of the nanoantennas associated with the excitation of surface plasmons along the nanorod axes. We demonstrate a very strong sensitivity of their resonant characteristics to both the presence of a dielectric load and the modification of the refractive index of this load. The spectral position of the nanoantenna resonance can be tuned throughout the visible spectral range from about 550 to 800 nm with a sensitivity better than 3 Å per 1 nm thickness of dielectric load. This allows for the development of metallodielectric composite materials with a tuneable op-

tical response throughout the whole visible spectral range by only changing the dielectric load for the same metallic host.

These dielectric-loaded plasmonic nanoantenna arrays are a type of anisotropic metallodielectric metamaterials with fully adjustable optical properties. The optical properties are determined not by the individual nanorods but the assembly and as such, are governed by the electromagnetic interaction between the nanorods in the array, which can be tuned by introducing dielectric material between the rods. Such metamaterials can be used to develop new nonlinear optical materials with enhanced effective nonlinear susceptibility utilizing the field enhancement effects of the nanoantennas. They can act as optical sensors with the sensitivity and working spectral range dependent on both the dielectric load thickness and the permittivity of the adsorbate. Such nanorod arrays are inexpensive to fabricate and are required for many applications in surface enhanced Raman scattering, sensing, optical nonlinearity enhancement, and negative refraction development at visible wavelengths.

II. EXPERIMENT

The plasmonic nanoantenna arrays were fabricated using electrochemical deposition into a template of anodized aluminum oxide (AAO).¹⁷ The template is made of an aluminum (Al) film that is sputter deposited onto a glass substrate covered with a 5-nm-thick Au film. The anodisation process consists in the electrochemical conversion of Al in Al₂O₃ which leads to the formation of a quasiperiodic array of nanopores due to a self-organization process. The electrochemical conditions (electrolyte and applied voltage) are chosen to control both the nanopore size and separation. Nanoporous AAO templates are then used as a template for the electrochemical growth of Au into the nanopores. The diameter of the Au nanorods is then determined by the pore size while their length can be varied by controlling the electrodeposition time with maximum length determined by the thickness of the AAO layer. The AAO matrix can subsequently be removed chemically using aqueous sodium hydroxide (NaOH) leaving the array of oriented Au nanorods

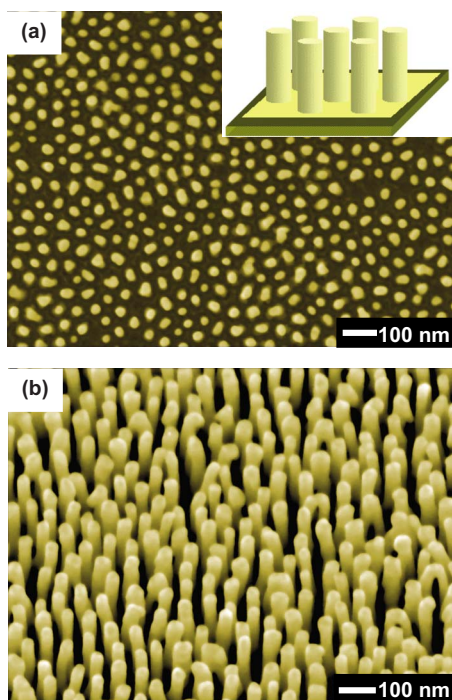


FIG. 1. (Color online) SEM images of nanorod arrays: (a) plan view of the nanorods in the AAO matrix (the rod cross sections looks irregular due to the small random tilt of the nanorods), (b) angle-view of the bare nanorod arrays after matrix removal.

embedded in air, and standing on the substrate (Fig. 1). The nanorods were then covered with a 3BCMU (poly-3-butoxy-carbonyl-methyl-urethane polydiacetylene) film by spin-coating the monomer solution (50 mg of monomer for 5 ml of CHCl_3) onto the array of bare rods. The thickness of the monomer/polymer film was characterized using atomic force microscopy and shown to vary from a few tens to a few hundreds of nanometers, and can be smaller than the nanorod length. The resultant nanorod-monomer composite was studied for various monomer thicknesses and various degrees of monomer photopolymerization.

III. RESULTS AND DISCUSSION

A. Optical properties of partially coated nanorod arrays

The extinction spectra of the nanoantenna arrays embedded in AAO (before removal of AAO matrix) measured with *s*- and *p*-polarized incident light (the electric field is perpendicular or has a component parallel to the nanorod long axis, respectively) is dominated by two peaks (Fig. 2) which reflect both the anisotropy of the array and the coupling between the rods. The short-wavelength peak located around 525 nm is related to the surface plasmon excitation perpendicular to the nanorod long axis. We refer to this resonance as transverse (*T*) resonance, which may be excited using either *s*- or *p*-polarized incident light. The long-wavelength peak appears only under obliquely incident *p*-polarized excitation light and is the longitudinal (*L*) resonance associated with the electron plasma movement along the nanorod long

axes. Due to the electromagnetic interaction between the nanorods in the array, this peak is related to a collective resonance of the array originating from the dipolar coupling of the plasmonic resonances of individual nanorods with the dipoles of the neighboring rods aligned parallel (the antiparallel alignment is not generally optically active).¹⁸ The interaction leads to a significant short-wavelength shift of the position of the *L* resonance of the array compared to the long-axis resonance wavelength of an isolated nanorod of similar aspect ratio. (The longitudinal resonance wavelength for an individual nanorod can be calculated to be $\lambda_{\text{ind}} \approx 1760 \text{ nm}$.¹⁶) The position of these resonances can therefore be controlled by changing not only the size of the nanorods (length and diameter) but also their spacing, which by itself strongly affects the spectral position of the *L* resonance.^{18,19} The *T* and *L* resonances can be easily identified due to their dependence on the angle of incidence. With the increase of the incident angle, the amplitude of the *L* resonance increases due to the increase of the component of the electric field parallel to the long axis of the nanorod.

Upon removal of the AAO matrix, exposing the nanorods to air, the change of the surrounding's refractive index from $n=1.6$ to 1 shifts the *L* resonance towards the *T* resonance position as should be expected.^{16,19} For the nanorod array parameters under consideration, the coupling leads to the situation when the two resonances are significantly overlapped and can only be distinguished by the angular-dependent extinction amplitude of the *L* resonance using *p*-polarized light [Fig. 2(b)]. Embedding the nanorods into a layer of 3BCMU monomer ($n=1.46$) shifts the *L*-peak position towards the one observed for nanorods in the AAO matrix due to the intermediate refractive index of mono-3BCMU compared to air and AAO.

An interesting effect is observed when only part of the rods is covered with the dielectric [Fig. 2(c)]. As the thickness of a dielectric deposited onto the array increases, the longitudinal resonance shifts towards the red to some intermediate position between the resonances of bare and fully covered nanorods. The extinction amplitude for partly covered nanorods is also intermediate between the two limiting coverages. Indeed, a gradual change in the dielectric layer thickness results in the modification of the spectral position of the resonances (Fig. 2): the dielectric acts as a load on the metallic nanoantenna analogous to loaded rf antennas.²⁰ Loading the antenna in this manner changes the impedance of the structure resulting in a shift of the antenna resonance through the sensitivity of the SPP wavelength to the refractive index of the adjacent dielectric. Hence, the optical properties of plasmonic nanoantennas can be modified by tuning the thickness and/or the refractive index of the dielectric load. The measured dependence of the *L*-resonance position on the load thickness is found to follow a fairly linear variation in the spectral range considered [Fig. 2(d)]. This behavior is in agreement with the simple model based on a dielectric-loaded metallic nanoantenna discussed below.

Radio-frequency linear antenna of finite length can be excited with the electric field polarized along their length at the resonant frequencies corresponding to standing electromagnetic waves in the linear wire: $\omega/c = q = m\pi/L$, where L is the rod length, m is an integer, q and ω are the wave vector and

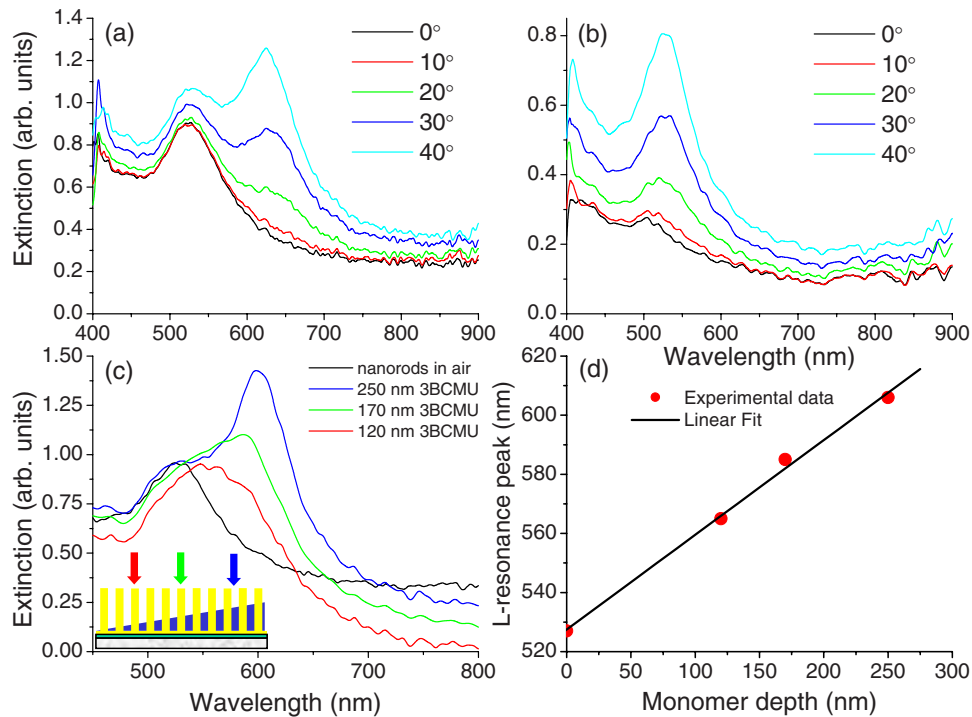


FIG. 2. (Color online) Extinction spectra of the nanorods in (a) AAO matrix and (b) bare nanorods (matrix removed) measured at different angles of incidence for p polarization of the incident light. The nanorod length, diameter, and separation are 300, 25, and 40 nm, respectively. (c) Extinction spectra of the nanorods covered with monomer of different thickness as shown in the inset for 40° angle of incidence: 0, 120, 170, and 250 nm. (d) The dependence of the L -resonance position on the polymer thickness plotted from (c): (circles) experiment, (line) the model of dielectric-loaded plasmonic antenna (the absolute value of the peak position is normalized to the experimental data).

frequency of the excitation wave, respectively.²⁰ For a metallic wire at optical frequencies, this condition should be rewritten taking into account the eigenmodes of the metallic wire; namely, surface plasmon excitations $q = k_{\text{SP}}$, where k_{SP} is the surface plasmon polariton (SPP) wave vector.²¹ In the case of a wire of circular cross section, these are cylindrical surface plasmons with frequency determined by the nanowire size, shape, material, and the surrounding's dielectric constant.^{22,23} In the situation considered experimentally, the distance between antennas is smaller than the surface plasmon field extension around the nanorod ($l \ll 1/\kappa_{\text{SP}}$), thus their optical properties can no longer be rigorously described by the dipolar response associated with isolated nanorods. However, a simplified description of a plasmonic nanoantenna can be achieved considering standing waves of SPPs on the metal/dielectric interface of the wires. For a dielectric-loaded nanoantenna of length L , the resonance conditions can be expressed adopting the antenna description as $k_{\text{SP}}^{(1)}L_1 + k_{\text{SP}}^{(2)}L_2 = m\pi$, where L_1 is the length of the loaded part of the antenna, $L_2 = L - L_1$, $k_{\text{SP}}^{(i)}$ is the surface plasmon wave vector on the metal-dielectric ($i=1$) and metal-air ($i=2$) interfaces, and m is a positive integer. This model predicts a linear dependence of the loaded-antenna resonances in the visible spectral range for Au nanorods.

The experimentally observed sensitivity of the L resonance with respect to the dielectric thickness is $\Delta\lambda/\Delta h \approx 3 \text{ \AA}/\text{nm}$ for the 300 nm long nanoantenna (diameter 25 nm, spacing in the array 40 nm, and the dielectric with

$n=1.46$). The estimation of the sensitivity is based on the maximum achievable shift of the resonant wavelength of the nanorod array (the resonant wavelength when the nanorods are completely in air and the resonant wavelength when they are completely covered with a dielectric). The resonance positions for the intermediate thickness of a monomer confirm this estimation exhibiting a linear dependence of the L -mode position on the dielectric thickness [Fig. 2(d)]. This sensitivity, however, depends on the nanorod array parameters and will be different for different nanorod length, thickness, and separation. It increases for longer nanorods and larger nanorod separations. On the other hand, the arrays with a significant distance between nanorods are more difficult to fabricate (nanorod diameter and spacing are coupled together due to the self-organization nature of the template fabrication). A smaller number of nanorods under optical interrogation also leads to a lower signal-to-background ratio of the measurements in this case. Moreover, if the coupling between the nanorods is small, the dipolar resonances of the nanorods are not sensitive to the dielectric coverage if the thickness is around half the nanorod length.

The electromagnetic interaction between nanorods has not been taken into account in the simple analytical model described above. However, this interaction results in a significant modification of the electromagnetic field distribution in the antenna arrays and related modification of the plasmonic resonances of the antennas. We used finite element numerical calculations on a model system consisting of a square array of Au nanorods embedded in a dielectric load of varying

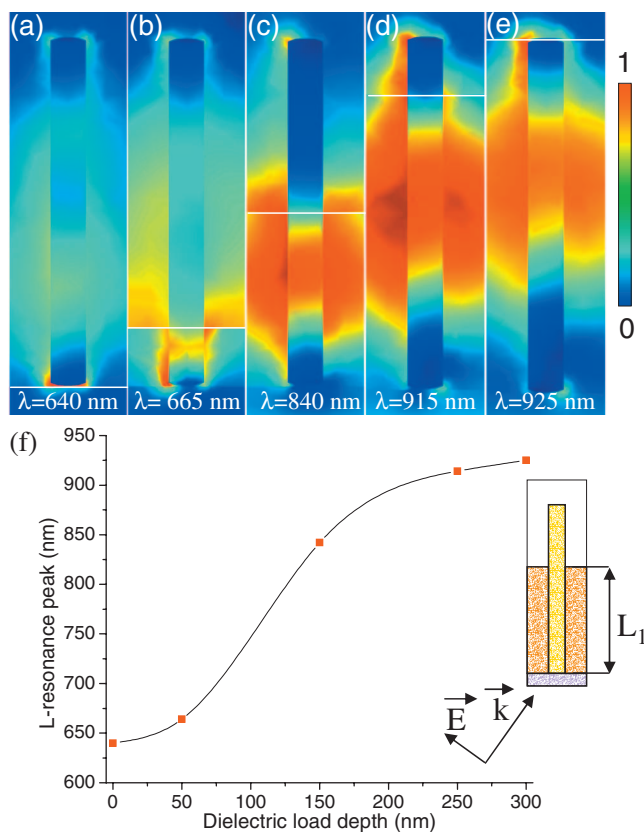


FIG. 3. (Color) Electric field amplitude distributions in the primitive cell of the periodic nanorod array at the longitudinal resonance in the case of (a) bare, dielectric-loaded, (b) 50, (c) 150, (d) 250 nm, and (e) fully coated nanorods. The color scale is independent for each distribution. The nanorod length, diameter, and separation are 300, 30, and 100 nm, respectively. The numerical modeling is based on finite-element method. (f) Dependence of the L -mode spectral position on the load thickness in the model system. The inset shows the illumination geometry.

thickness to illustrate the observed behavior (Fig. 3). A strongly modified field distribution is observed in the nanorod array compared to the dipolar response expected for isolated nanorods, with the electric field concentrated between the nanorods and not at their extremities as one would expect for an isolated dipolar antenna. This is in agreement with the calculated dependence of the L -mode position in the model system on the load thickness [Fig. 3(f)]. The spectral sensitivity of the L -resonance is highest for a dielectric coverage varying in the 50–250 nm thickness range (for the 300 nm long nanorods) for which the influence of the dielectric on the field distribution is most significant, a behavior that is also observed in the experiments (Fig. 2). The spectral sensitivity of the L resonance is lower for either very thin or thick load due to the low electric field at the antenna extremities. This is the result of the rod-to-rod interaction in the array and the reason for the calculated nonlinear dependence of the L -resonance position in contrast to the linear dependence predicted by the model of individual nanoantenna. The spectral sensitivity estimated from the linear part of the calculated dependence in Fig. 3 is almost $10 \text{ \AA}/\text{nm}$ for the nanoantennas under consideration. (Please note that the ex-

periment where linear behavior is observed has been performed for the sample parameters corresponding to the central part of the dependence where it is almost linear.) Thus, the L resonance of the nanoantenna array is extremely sensitive to the thickness of the dielectric coverage. This effect can be used to adjust the L -resonance position in the desired spectral range and still have a bare part of the nanorods available for further use as a sensing element.

B. Influence of the modification of the dielectric host

To demonstrate the sensitivity of the L resonance of the nanorod array to the refractive index of the dielectric load, we have studied the polymerization process of mono-3BCMU around the nanorods. The nanoantenna array (length 300 nm, diameter 20 nm, spacing 40 nm) was fully covered with the monomer the fractional polymerization of which causes a net change of the refractive index of the load. Figure 4 shows the extinction spectra of the metallodielectric composite before and following UV irradiation, used as an actinide source. After photopolymerization, the extinction spectrum of the metallodielectric composite resolves two additional absorption peaks at 580 and 625 nm associated with the formation of the polymer.²⁴ This is highlighted in Fig. 4(b) which shows the change in extinction during the UV polymerization process. Here the absorption peaks related to the polymer are clearly observed with an additional shift in the position of the L -resonance extinction peak of the antenna array. The spectra in Fig. 4(b) show the increase in absorption (highlighted by the blue box) and the changes in extinction due to the shift of the resonance wavelength (highlighted by the red box) as the photopolymerization time increases from 0 to 8 min. Noise in this figure is a result of narrow bandwidth emission lines in the spectral output of the UV light source used for polymerization. The final position of the L resonance is shifted to longer wavelengths by about 25 \AA . The direction of this shift is consistent with the increased refractive index of the polymer compared to the monomer (the large birefringence of poly-3BCMU depends on alignment but typically $n_{\perp} \approx 1.635$ and $n_{\parallel} \approx 1.535$ have been measured²⁴). From these measurements, the polymer mass fraction is estimated to be ~ 0.01 in the sensitive region of nanorods.²⁵

Photochromic modification of the polymer-nanorod composite was studied under picosecond illumination at 515 nm addressing the T resonance of the array associated with the short axes of the nanorods. At moderate illumination intensities (up to $2.8 \text{ W}/\text{cm}^2$), additional polymerization occurs as is evidenced by the increase in the optical absorption associated with the polymer formation, no significant L -peak shift is observed. However, at higher illumination intensities [Figs. 4(c) and 4(d)], the shift of the longitudinal resonance peak does occur and is related to the spatial overlap of the field distributions associated to both L and T resonances. The nature of this shift is related mainly to induced nonreversible photochromic modifications of the polymer. In addition, a reversible shift of the L mode is observed when the light is switch on/off from its maximum intensity indicating the presence of nonlinear optical effects leading to the refractive

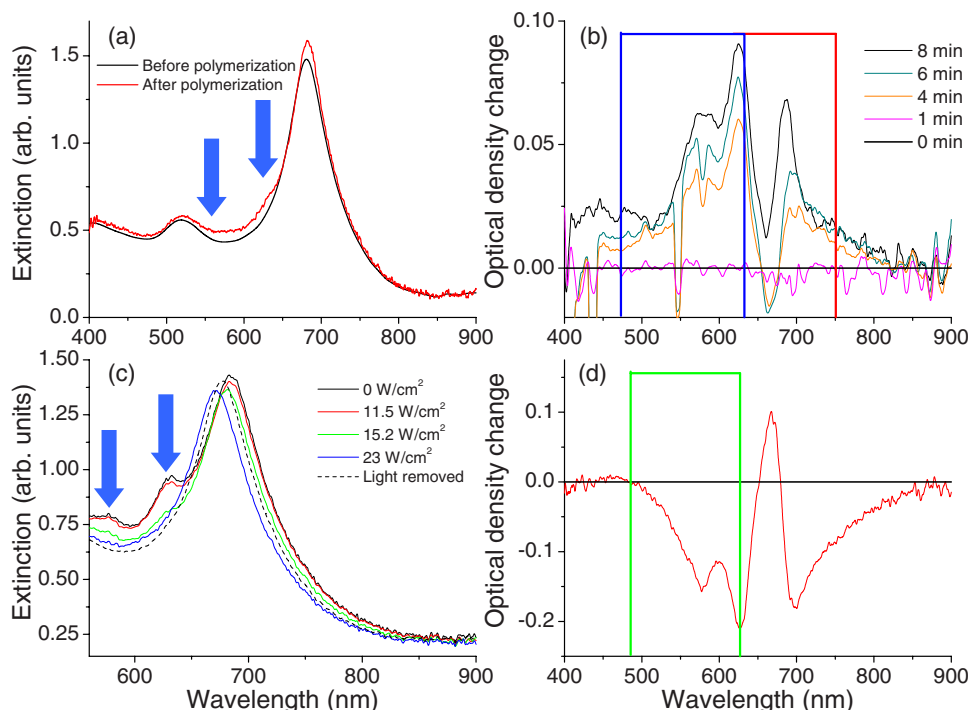


FIG. 4. (Color online) (a) Extinction spectra of nano-antenna-dielectric composite before and after UV photopolymerization. (b) The changes of the extinction due to polymerization when the illumination time varies from 0 to 8 min. The polymer signature is evidenced by additional absorption (shown by the blue box) and the change in position of the L -resonance peak (shown by the red box). (c) Extinction spectra after polymer exposure to 515 nm control light of different intensities. (d) The change in the extinction spectrum after irradiation of polymer with 515 nm light plotted from (c). Photobleaching is shown by the green box. The nanorod length, diameter, and separation are 300, 20, and 40 nm, respectively.

index change of the dielectric host under illumination near the transverse resonance wavelength.

Exposing the photopolymer to increasing actinide powers eventually leads to the photobleaching of the species. The associated decrease in refractive index is observed as a 9 nm blueshift of the L resonance in the spectrum of Fig. 4. This photochromic effects can be useful for optical data storage applications and all-optical switching in the nanorod-polymer systems.

Thus, plasmonic nanoantenna resonances are very sensitive to changes of the refractive index of the polymer matrix. The competing effects of polymerization and photobleaching of the polymerized material can be reliably distinguished by examining the behavior of the optical response of the nanoantenna array. The load of the nanoantenna array can be changed by modifying the spatial distribution of the dielectric between the nanorods. This modifies not only the resonances of the individual nanorods in the array but also the interaction strength between them.

IV. CONCLUSION

We have fabricated and studied the optical properties of dielectric-loaded plasmonic nanoantenna arrays with strongly interacting, oriented Au nanorods standing on a

transparent substrate. The resonant response of the arrays can be tuned throughout the whole visible spectral range with high precision by changing the dielectric load thickness and refractive index. The recorded sensitivity was measured to be better than 3 Å/nm.

Such nanoantenna arrays can be considered as a type of inhomogeneous metallo-dielectric metamaterials with fully adjustable optical properties thus suitable for applications ranging from optical sensing to spectroscopic experiments, as well as for the development of new nonlinear metamaterials with enhanced effective nonlinear susceptibility due to the electromagnetic field enhancement. The proposed approach allows one to achieve, in a single array of nanorods, the continuous tuning of the nanoantenna resonances to cover the whole visible range. This has therefore potential applications in sensing, field-enhanced fluorescence, Raman scattering, and second-harmonic detection of the species with *a priori* unknown resonant wavelengths. Additionally, the fabrication process for these systems is inexpensive and scalable, which provides great prospect for their future use in practical device applications.

ACKNOWLEDGMENTS

This work was supported, in part, by EPSRC (UK) and EU FP6 Network of Excellence Plasm Nano-Devices.

- ¹L. M. Tong, R. R. Gattass, J. B. Ashcom, S. L. He, J. Y. Lou, M. Y. Shen, I. Maxwell, and E. Mazur, *Nature (London)* **426**, 816 (2003).
- ²D. Sirbully, M. Law, H. Yan, and P. Yang, *J. Phys. Chem. B* **109**, 15191 (2005).
- ³M. S. Gudiksen, L. J. Lauhon, J. Wang, D. C. Smith, and C. M. Lieber, *Nature (London)* **415**, 617 (2002).
- ⁴Y. Cui, Q. Wei, H. Park, and C. M. Lieber, *Science* **293**, 1289 (2001).
- ⁵P. Mühlischlegel, H.-J. Eisler, O. J. F. Martin, B. Hecht, and D. W. Polh, *Science* **308**, 1607 (2005).
- ⁶G. Schider, J. R. Krenn, A. Honehau, H. Ditlbacher, A. Leitner, F. R. Aussenegg, W. L. Schaich, I. Puscasu, B. Monacelli, and G. Boreman, *Phys. Rev. B* **68**, 155427 (2003).
- ⁷K. Ueno, V. Mizeikis, S. Juodkazis, K. Sasaki, and H. Misawa, *Opt. Lett.* **30**, 2158 (2005).
- ⁸V. Podolskiy, A. Sarychev, and V. Shalaev, *J. Nonlinear Opt. Phys. Mater.* **11**, 65 (2002).
- ⁹A. Ono, J. I. Kato, and S. Kawata, *Phys. Rev. Lett.* **95**, 267407 (2005).
- ¹⁰G. Schider, J. R. Krenn, W. Gotschy, B. Lamprecht, H. Ditlbacher, A. Leitner, and F. R. Aussenegg, *J. Appl. Phys.* **90**, 3825 (2000).
- ¹¹C. Reinhardt, S. Passinger, B. N. Chichkov, W. Dickson, G. A. Wurtz, P. Evans, R. Pollard, and A. V. Zayats, *Appl. Phys. Lett.* **89**, 231117 (2006).
- ¹²G. Sauer, G. Brehm, S. Schneider, H. Graener, G. Seifert, K. Nielsch, J. Choi, P. Goring, U. Gosele, P. Miclea, and R. B. Wehrspohn, *J. Appl. Phys.* **97**, 024308 (2005).
- ¹³V. A. Podolskiy, A. K. Sarychev, and V. M. Shalaev, *Opt. Express* **11**, 735 (2003); V. M. Shalaev, W. Cai, U. Chettiar, H.-K. Yuan, A. K. Sarychev, V. P. Drachev, A. V. Kildishev, *Opt. Lett.* **30**, 3356 (2005).
- ¹⁴V. A. Podolskiy, A. K. Sarychev, E. E. Narimanov, and V. M. Shalaev, *J. Opt. A, Pure Appl. Opt.* **7**, S32 (2005).
- ¹⁵M. G. Silveirinha, P. A. Belov, and C. R. Simovski, *Phys. Rev. B* **75**, 035108 (2007).
- ¹⁶C. F. Bohren, D. R. Huffman, *Absorption and Scattering of Light by Small Particles* (Wiley, New York, 1983).
- ¹⁷P. Evans, W. R. Hendren, R. Atkinson, G. A. Wurtz, W. Dickson, A. V. Zayats, and R. J. Pollard, *Nanotechnology* **17**, 5746 (2006).
- ¹⁸R. Atkinson, W. R. Hendren, G. A. Wurtz, W. Dickson, A. V. Zayats, P. Evans, R. J. Pollard, *Phys. Rev. B* **73**, 235402 (2006).
- ¹⁹P. R. Evans, G. A. Wurtz, R. Atkinson, W. Hendren, W. Dickson, R. J. Pollard, and A. V. Zayats, *J. Phys. Chem. C* **111**, 12522 (2007).
- ²⁰C. Balanis, *Antenna Theory: Analysis and Design* (Wiley, New York, 1997).
- ²¹A. V. Zayats, I. I. Smolyaninov, and A. A. Maradudin, *Phys. Rep.* **408**, 131 (2005).
- ²²C. A. Pfeiffer, E. N. Economou, and K. L. Ngai, *Phys. Rev. B* **10**, 3038 (1974).
- ²³M. I. Haftel, C. Schlockermann, and G. Blumberg, *Appl. Phys. Lett.* **88**, 193104 (2006).
- ²⁴W. A. Pender, A. J. Boyle, P. Lambkin, W. J. Blau, K. Mazheri, D. J. Westland, V. Skarda, and M. Sparpaglione, *Appl. Phys. Lett.* **66**, 7 (1995).
- ²⁵X.-Y. Zhang, Q. Li, J.-Z. Liu, and S. Sottini, *J. Photochem. Photobiol., A* **95**, 239 (1996).